

# Shape optimization approach for sharp-interface reconstructions in time-domain full waveform inversion

Antoine Laurain

Instituto de Matemática e Estatística, Universidade de São Paulo.

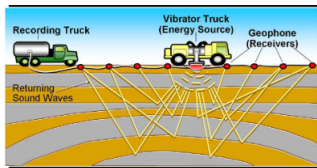
*joint work with K. J. Roberts and Y. F. Albuquerque*

IFIP TC7 2021

We gratefully acknowledge support of the RCGI - Research Centre for Gas Innovation, hosted by the University of São Paulo (USP) and sponsored by FAPESP - São Paulo Research Foundation (2014/50279-4), ANP and Shell Brasil.

# Seismic imaging

- ▶ Produce images of the subsurface of the Earth by processing seismic reflection data created by natural or artificial sources and collected at receivers at the surface.
- ▶ Data is produced by sending acoustic/elastic waves generated by controlled sources at the surface into the medium and recording the reflection waves at receivers (geophones) also located at the surface.
- ▶ Applications: imaging the lithosphere, imaging glaciers, subsurface structures in volcanic area, detect ocean's internal tides, hydrocarbon exploration ...



# Sharp-interface models for salt geometry inversion

[Lewis, Vigh 2016] *“Salt bodies have a sharp velocity contrast to the sediment velocities at their boundaries and very irregular geometries, any errors in the location of the salt boundaries in the model will lead to a much larger error in the waves traveling through them.”*

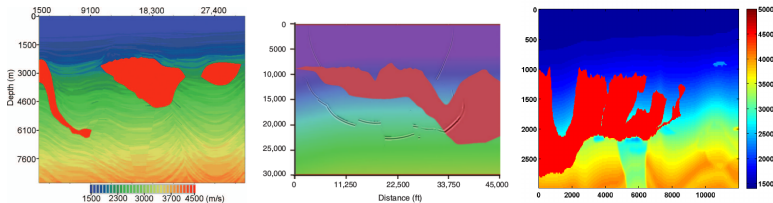


**Figure:** Pluto velocity model (left), Sigsbee2a velocity model (center) top left portion of BP2004 velocity model (right)

# Acoustic wave equation

- ▶ 2D acoustic wave equation with **Perfectly Matched Layer (PML)** from [Grote and Sim 2010], [Kaltenbacher et al. 2013], used to model a semi-infinite domain and suppress parasitic wave reflections.

$$\partial_{tt}^2 u + \text{tr } \Psi_1 \partial_t u + \text{tr } \Psi_2 u - \nabla \cdot (c^2 \nabla u) - \nabla \cdot \mathbf{p} = c^2 f, \text{ in } \mathcal{D} \times [0, T]$$

$$\partial_t \mathbf{p} + \Psi_1 \mathbf{p} + \Psi_2 (c^2 \nabla u) = 0 \text{ in } \mathcal{D} \times [0, T],$$

$$u|_{t=0} = 0 \text{ in } \mathcal{D},$$

$$\partial_t u|_{t=0} = 0 \text{ in } \mathcal{D},$$

$$\mathbf{p}|_{t=0} = 0 \text{ in } \mathcal{D},$$

$$\partial_t u + c \nabla u \cdot \mathbf{n} = 0 \text{ on } \Gamma \times [0, T]$$

$$\mathbf{p} \cdot \mathbf{n} = 0 \text{ on } \Gamma \times [0, T]$$

- ▶  $\mathcal{D} \subset \mathbb{R}^2$  is a rectangle with boundary  $\Gamma$ .
- ▶  $c$  is the P-wave velocity.
- ▶  $f$  is a source term.
- ▶  $\Psi_1, \Psi_2$  are damping matrices.

# Sharp-interface model

- ▶  $c = c_0\chi_\Omega + c_1\chi_{\mathcal{D}\setminus\Omega}$  and  $c_0, c_1 : \mathcal{D} \rightarrow \mathbb{R}$  are Lipschitz functions.
- ▶  $\chi_\Omega(x) = 1$  for  $x \in \Omega$  and  $\chi_\Omega(x) = 0$  for  $x \in \mathcal{D} \setminus \Omega$ .
- ▶ the unknown interface is the boundary of  $\Omega$

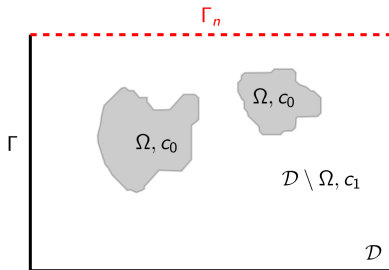


Figure: Wave velocity  $c = c_0\chi_\Omega + c_1\chi_{\mathcal{D}\setminus\Omega}$ . Measurements on  $\Gamma_n$ .

# Shape optimization approach for FWI

- ▶ Shape optimization approach:

$$\text{minimize } J(\Omega) = \frac{1}{2} \sum_{i=1}^{N_s} \sum_{j=1}^{N_m} \int_0^T (u_i(x_j, t) - d_i(x_j, t))^2 dt,$$

- ▶  $c = c_0 \chi_{\Omega} + c_1 \chi_{\mathcal{D} \setminus \Omega}$  is piecewise Lipschitz and the minimization variable is the geometry  $\Omega$ .
- ▶  $\{f_i\}_{i=1}^{N_s}$  is a given set of sources (shots).
- ▶  $u_i$  is the acoustic pressure corresponding to  $f_i$ ,  $u_i$  depends on  $\Omega$  through  $c$ .
- ▶  $d_i(x_j, \cdot)$  denotes the seismogram corresponding to the source  $f_i$  and the receiver at  $x_j$ .
- ▶  $c_0$  and  $c_1$  can be given or unknown functions, depending on the application.

# Sharp-interface models for salt geometry inversion

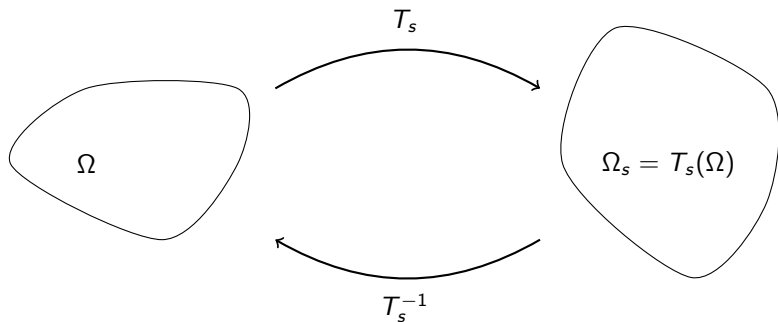
- ▶ Tikhonov regularization tends to produce smooth velocity models, which precludes the reconstruction of singular features such as sharp interfaces, discontinuities, and high contrasts.
- ▶ An accurate representation of the salt body interface may considerably improve the quality of the images.
- ▶ The incorporation of prior information about sharp interfaces and high contrast explicitly in the modeling of the problem is especially advantageous for inverse problems (regularization effect).

# Finite elements or finite differences?

- ▶ Traditionally, FWI is solved using finite difference methods (FDM) with structured grids, which is convenient for large-scale problems and explicit time-stepping.
- ▶ The finite difference approach has been studied in:  
*Level set-based shape optimization approach for sharp-interface reconstructions in time-domain full waveform inversion*  
Y. F. Albuquerque, A. Laurain, I. Yousept,  
SIAM Journal on Applied Mathematics, 81(3), 939-964, (2021)
- ▶ The sharp interface of the salt body is irregular in shape and therefore requires relatively fine structured grid resolution to accurately resolve using FDM.
- ▶ Finite element methods (FEM) permit the usage of variable unstructured meshes that can more efficiently model these sharp interfaces.
- ▶ We rely on a distributed expression of the shape derivative which is more accurate than a boundary expression using FEM.

# Shape derivative

- ▶  $T_s : \mathcal{D} \rightarrow \mathcal{D}$  is a given diffeomorphism, with  $\Omega_s := T_s(\Omega) \subset \mathcal{D}$ .
- ▶  $J(\Omega_s)$  is a shape functional.
- ▶ **Shape derivative:**  $dJ(\Omega)(\theta) = \lim_{s \searrow 0} \frac{J(\Omega_s) - J(\Omega)}{s}$
- ▶ Velocity  $\theta = \partial_s T_s|_{s=0}$
- ▶ Example:  $T_s(x) = (I + s\theta)(x)$  for  $s \in [0, \tau]$ .



# Shape derivative for FWI

- ▶ Cost functional for FWI:

$$J(\Omega) = \frac{1}{2} \sum_{i=1}^{N_s} \sum_{j=1}^{N_m} \int_0^T (u_i(x_j, t) - d_i(x_j, t))^2 dt.$$

- ▶  $d_i$  are the seismograms and  $x_j$  the receiver positions.
- ▶ **Distributed shape derivative** given by:

$$dJ(\Omega)(\theta) = \int_{\mathcal{D}} \mathbf{S}_1 : D\theta + \mathbf{S}_0 \cdot \theta,$$

$$\mathbf{S}_1 = \int_0^T [-\partial_t u \partial_t u^\dagger + c^2 \nabla u \cdot \nabla u^\dagger] I_n - c^2 (\nabla u \otimes \nabla u^\dagger + \nabla u^\dagger \otimes \nabla u) dt,$$

$$\mathbf{S}_0 = \int_0^T (2c \nabla u \cdot \nabla u^\dagger) \tilde{\nabla} c.$$

- ▶  $\tilde{\nabla} c(x) := \nabla c_0(x) \chi_\Omega(x) + \nabla c_1(x) \chi_{\mathcal{D} \setminus \Omega}(x) \neq \nabla c(x)$ .

# Adjoint state equation

- ▶ Optimize-then-discretize approach (the adjoint state is computed in the continuous domain).
- ▶ The adjoint for the modified acoustic wave equation is given by:

$$\begin{aligned} \partial_{tt}^2 u^\dagger - \text{tr } \Psi_1 \partial_t u^\dagger + \text{tr } \Psi_2 u^\dagger - \nabla \cdot (c^2 \nabla u^\dagger) - \nabla \cdot (c^2 \Psi_2 \boldsymbol{\rho}^\dagger) \\ = - \sum_{j=1}^{N_m} [u(x_j) - d(x_j)] \text{ in } \mathcal{D} \times [0, T], \\ -\partial_t \boldsymbol{\rho}^\dagger + \Psi_1 \boldsymbol{\rho}^\dagger + \nabla u^\dagger = \mathbf{0} \text{ in } \mathcal{D} \times [0, T], \\ u^\dagger|_{t=T} = 0 \text{ in } \mathcal{D}, \\ \partial_t u^\dagger|_{t=T} = 0 \text{ in } \mathcal{D}, \\ \boldsymbol{\rho}^\dagger|_{t=T} = \mathbf{0} \text{ in } \mathcal{D}, \\ -\partial_t u^\dagger + c \Psi_2 \boldsymbol{\rho}^\dagger \cdot \mathbf{n} + c \nabla u^\dagger \cdot \mathbf{n} = 0 \text{ on } \Gamma \times [0, T] \\ \boldsymbol{\rho}^\dagger \cdot \mathbf{n} = 0 \text{ on } \Gamma \times [0, T] \end{aligned}$$

- ▶ To get a descent direction  $\theta$  for the optimization problem, we solve (for  $\theta$ ) an elliptic PDE using finite elements:

$$\begin{aligned} \int_{\mathcal{D}} \alpha_1 g D\theta : D\xi + \alpha_2 g \theta \cdot \xi &= -dJ(\Omega)(\xi) \\ &= - \int_{\mathcal{D}} \mathbf{S}_1 : D\xi + \mathbf{S}_0 \cdot \xi \quad \text{for all } \xi \in (H_0^1(\mathcal{D}))^2 \end{aligned}$$

- ▶ Here  $g > 0$  is a weight function.

- ▶ Shape is represented with an indicator function:  $\chi : \mathcal{D} \times [0, s_0] \rightarrow \mathbb{R}$ , equal to 1 for points inside the salt body and 0 outside.
- ▶ Shape updates are obtained by solving the transport equation to advect  $\chi$  for a fixed number of pseudo-timesteps ( $\mathcal{O}(10)$ ):

$$\partial_s \chi + \boldsymbol{\theta} \cdot \nabla \chi = 0 \text{ in } \mathcal{D} \times [0, s_0], \quad (1)$$

in which  $\boldsymbol{\theta}$  is the descent direction.

- ▶ (1) was solved for 10 pseudo-timesteps (value selected through trial and error).
- ▶ (1) was discretized in space using a  $0^{th}$  order discontinuous Galerkin (DG0) approach and a  $4^{th}$  order Runge-Kutta scheme was used to discretize in time.

# Implementation

- ▶ Built using spyro: Acoustic wave modeling in Firedrake
  - <https://github.com/krober10nd/spyro>
  - Functions to compute descent direction  $\theta$  and advect the indicator function  $\chi$ .
- ▶ In space:
  - For wave eq.: higher-order mass lumped elements ( $P < 5$ ).
  - For transport eq.:  $0^{th}$  order discontinuous Galerkin.
- ▶ In time:
  - For wave equation: central finite difference.
  - For transport equation: RK4.

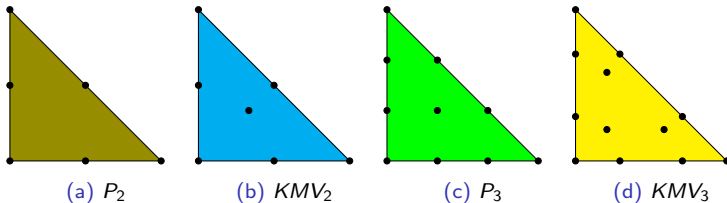
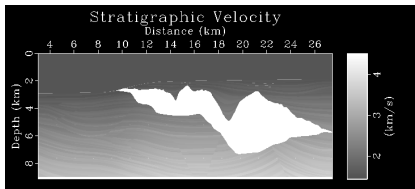


Figure: Some two-dimensional Lagrange and KMV elements

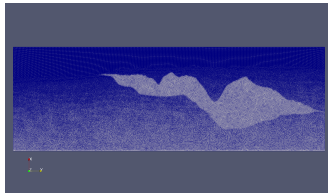


# Unstructured triangular meshes

- ▶ Developed with SeismicMesh:  
<https://github.com/krober10nd/SeismicMesh>.
- ▶ Variable resolution, graded triangular meshes adapted to P-wave field.



(a) A Sigsbee 2B stratigraphy model



(b) the model meshed with SeismicMesh

**Figure:** Example of meshing the Sigsbee 2B stratigraphy model.

# Numerical results - EAGE Salt

- ▶ First we test our implementation with a 2D slice of the EAGE model.
- ▶ 20 shots, 400 receivers, 3 seconds, 2 Hz noiseless Ricker wavelet

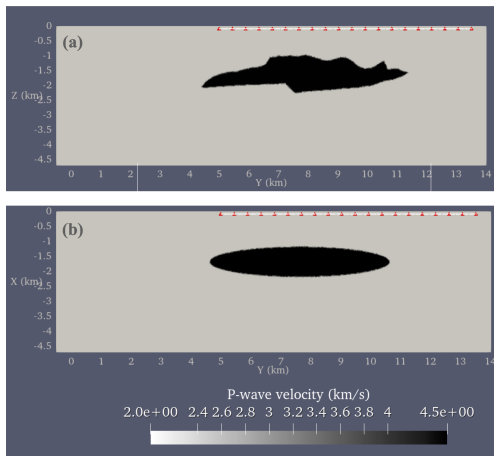


**Figure:** (a) target model, (b) starting model. A slice of the EAGE Salt model simplified to two velocities. Sources and receivers are shown in (a),(b).

# Numerical results - EAGE Salt

- ▶ After 5 hours and 83 iterations on 20 cores.
- ▶ Cost functional exhibited a three order of magnitude reduction from  $1.53e - 05$  at the first iteration to  $7.05e - 08$  at the final iteration

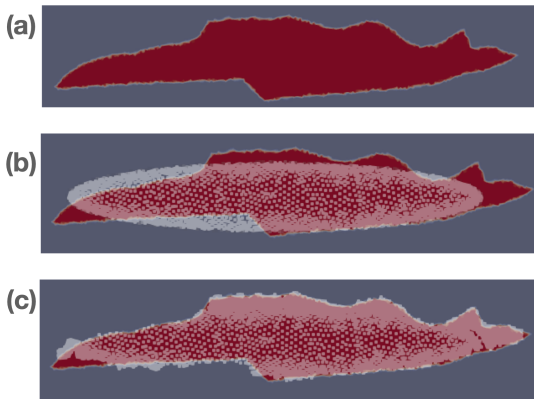
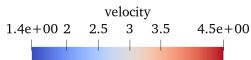
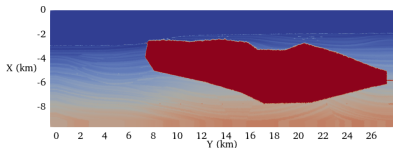


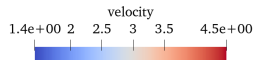
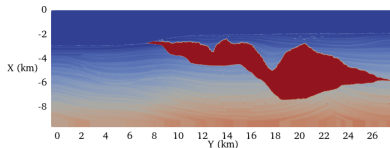
Figure: Optimization results for the EAGE problem.

# Numerical results - Sigbsee 2B stratigraphy

- ▶ The major difference in this case is the background velocity is non-constant.
- ▶ 120 shots, 1000 receivers, 2 Hz noiseless Ricker integrated for 7 seconds.



(a) guess model.

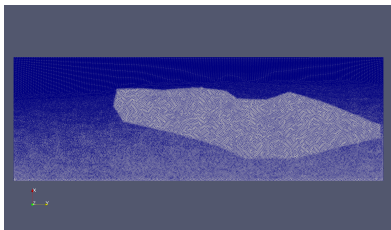


(b) target model.

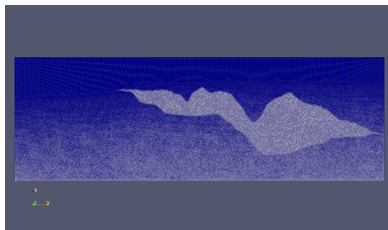
Figure: Sigbsee2b stratigraphy problem.

# Numerical results - Sigsbee 2B stratigraphy

- ▶ The ground truth simulations are conducted on the mesh of the target model and the inversion uses the mesh of the guess model.



(a) mesh of the guess model.



(b) mesh of the target model.

Figure: Meshes of the Sigsbee 2B stratigraphy model.

# Extended background velocity

- ▶ We use the background velocity of the Sigsbee 2B stratigraphy model and extend it inside the salt.
- ▶ The extension is such that sharp discontinuities do not appear near the salt body's interface with the background velocity field.
- ▶ The background velocity field is fixed throughout the optimization.

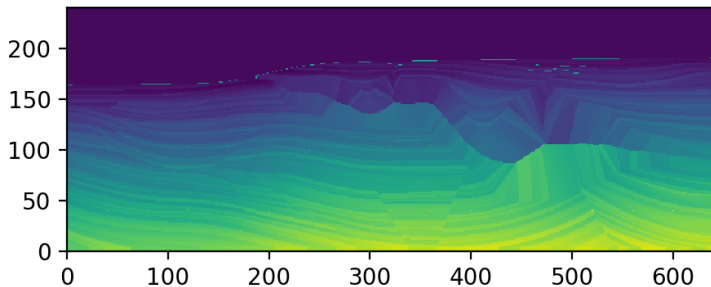


Figure: The extended background velocity field for the inversion.

# Numerical results - Sigsbee 2B stratigraphy

- ▶ 120 cores (one core per shot) to perform 96 iterations took 13 hours.
- ▶ Good agreement along the top of the salt body, little to no change on the bottom-of-the-salt.

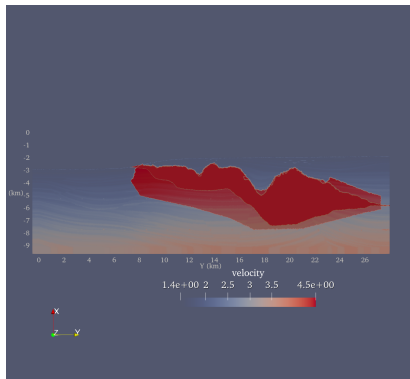


Figure: The final optimization result overlaid on the true velocity model.

- ▶ In this work we have considered a finite element approach with a PML formulation for the acoustic wave equation.
- ▶ The FE approach allows a more accurate representation of the salt body interface.
- ▶ Promising first results but the reconstruction needs to be improved at the bottom of the salt.
- ▶ The reconstruction of the background velocity will also be implemented.
- ▶ The finite difference approach has been studied in:  
*Level set-based shape optimization approach for sharp-interface reconstructions in time-domain full waveform inversion*  
Y. F. Albuquerque, A. Laurain, I. Yousept,  
SIAM Journal on Applied Mathematics, 81(3), 939-964, (2021)